Journal of Solid State Chemistry **150,** 112–120 (2000)
doi:10.1006/jssc.1999.8555, available online at http://www.idealibrary.com on IDEAL®

New $Yb_2Pt_3Sn_5$ Type Stannides

Dirk Kußmann, Rainer Pöttgen, and Gunter Kotzyba

Anorganisch-Chemisches Institut, Universität Münster, Wilhelm-Klemm-Strasse 8, D-48149 Münster, Germany
E-mail: pottgen@uni-muenster.de

Received August 10, 1999; in revised form October 12, 1999; accepted October 22, 1999

The stannides $CaErPt_3Sn_5$, $CaTmPt_3Sn_5$, $CaYbPt_3Sn_5$, and $CaLuPt_3Sn_5$ were prepared from the elements in glassy carbon crucibles under an argon atmosphere in a high-frequency furnace. Their $Yb_2Pt_3Sn_5$ type structure (space group *Pnma*) was refined from single-crystal X-ray data: $a = 736.4(1)$ pm, $b = 444.11(9)$ pm, $c = 2639.9(4)$ pm, w$R = 0.0905$, 1403 F^2 values, 63 variables for the erbium; $a = 733.9(2)$ pm, $b = 443.0(1)$ pm, $c = 2634.8(5)$ pm, w$R2 = 0.1430$, 1372 F^2 values, 63 variables for the thulium; $a = 733.9(1)$ pm, $b = 443.3(1)$ pm, $c = 2635.7(6)$ pm, w$R2 = 0.0734$, 2079 F^2 values, 64 variables for the ytterbium; and $a = 735.0(2)$ pm, $b = 441.6(2)$ pm, $c = 2634.1(7)$ pm, w$R2 = 0.1202$, 1344 F^2 values, 63 variables for the lutetium compound. The $Yb_2Pt_3Sn_5$ structure is built up from a complex threedimensional $[Pt_3Sn_5]$ polyanion in which the ytterbium atoms fill distorted hexagonal channels. The two crystallographically different ytterbium sites have coordination numbers (CN) 20 and 18, respectively. In the erbium, thulium, and lutetium compound, the CN 20 position is occupied exclusively by calcium atoms, while a mixed calcium–rare-earth occupancy is observed for the CN 18 position. In the ytterbium compound both positions show mixed occupancy. The refinements resulted in the compositions $Ca_{1.33}Er_{0.67}Pt_3Sn_5$, $Ca_{1.45}Tm_{0.55}Pt_3Sn_5$, $Ca_{1.28}Yb_{0.72}Pt_3Sn_5$, and $Ca_{1.63}Lu_{0.37}Pt_3Sn_5$ for the crystals investigated. These results were confirmed by magnetic susceptibility measurements. The erbium and the thulium compound show Curie–Weiss behavior with experimental effective magnetic moments of 9.5(2) and 8.4(2) μ_B, respectively. At 4.8(1) K, the erbium compound orders ferro- or ferrimagnetically, while antiferromagnetic ordering at $T_N = 5.0(1)$ K is observed for the thulium compound. $CaYbPt_3Sn_5$ shows Curie–Weiss behavior above 100 K with an experimental magnetic moment of 2.8(2) μ_B and $\Theta = -71(5)$ K, indicating mixed-valent behavior. $CaLuPt_3Sn_5$ shows a diamagnetic signal of -7.8×10^{-9} m³/mol. © 2000 Academic Press

***Key Words*: stannides; crystal structure; magnetism; mixed valence.**

INTRODUCTION

Intermetallic ytterbium compounds are interesting candidates in the search for valence change and/or mixed valent behavior, since the ytterbium atoms can adopt the configuration $[Xe]4f^{14}$ (Yb^{2+}) or $[Xe]4f^{13}$ (Yb^{3+}). A mixed valent behavior has been observed in the silicides Yb_3Si_5 (1, 2) and $YbPd_2Si_2$ (3), in several aluminides (4, 5), and recently also in the stannide $Yb_2Pt_3Sn_5$ (6). The latter has a peculiar crystal structure which is built up from a complex three-dimensional $[Pt_3Sn_5]$ polyanion in which the ytterbium atoms are embedded. The two crystallographically different ytterbium positions have coordination numbers (CN) 20, for Yb1, and 18, for Yb2. Magnetic susceptibility measurements revealed a magnetic moment of $\mu_{exp} = 2.6(1)$ μ_B/Yb, indicating mixed valency. In our previous investigation we assumed that the Yb2 atoms might be trivalent and occupy the smaller cage, while Yb1 is divalent and fills the larger cage, resulting in an approximate formulation ($Yb1^{2+}$) ($Yb2^{3+}$) $[Pt_3Sn_5]^{5-}$. Below 20 K the experimental magnetic moment of $Yb_2Pt_3Sn_5$ is only 1.0(1) μ_B/Yb, a situation frequently observed for divalent ytterbium (7–9). Thus, $Yb_2Pt_3Sn_5$ most likely contains exclusively divalent ytterbium at low temperature.

Recently we also obtained the calcium-based stannide $Ca_2Pt_3Sn_5$ (10), which is isotypic with the ytterbium compound. Here, both cation positions are definitely filled with a divalent cation. We have now extended our investigation with respect to quaternary compounds in order to study a possible site preference for a trivalent cation in the $Yb_2Pt_3Sn_5$ type structure. Herein we report on the new stannides $CaErPt_3Sn_5$, $CaTmPt_3Sn_5$, $CaYbPt_3Sn_5$, and $CaLuPt_3Sn_5$.

EXPERIMENTAL

Synthesis

Starting materials for the preparation of $CaErPt_3Sn_5$, $CaTmPt_3Sn_5$, $CaYbPt_3Sn_5$, and $CaLuPt_3Sn_5$ were calcium pieces (Johnson Matthey, $>99.5\%$, redistilled), ingots of the rare-earth elements ($>99.9\%$, Kelpin), platinum powder ($>99.9\%$, Degussa, 200 mesh), and a tin bar (99.9%, Heraeus).

The respective elemental components were mixed in the ideal atomic ratios 1:1:3:5, and the compounds were

0022-4596/00 $35.00

prepared by high-frequency melting (Hüttinger Elektronik, Freiburg, Typ TIG 1.5/300) of the elements in glassy carbon crucibles (SIGRADUR® G, glassy carbon, type GAZ006) under flowing argon. The argon was purified over titanium sponge (900 K), silical gel, and molecular sieves. The glassy carbon crucibles were placed in a water-cooled sample chamber (11). During the inductive heating process, the platinum powder and the tin pieces first form an alloy at low temperature, which finally reacts with the rare-earth metal and the calcium pieces in strongly exothermic reactions. Finally the ingots were annealed for about 2 h at ca. 1000 K. No weight losses were detected in the reactions, and all products could easily be separated from the glassy carbon crucibles by pounding at their base. No contamination of the samples was observed.

All samples were obtained in amounts of about 1000 mg. Compact pieces and powders of these stannides are stable in moist air. After an exposure time of several months no decomposition could be observed. The silvery single crystals of these stannides have metallic lustre and platelet-like shape. Powders are dark gray.

TABLE 1
Lattice Constants of Various $Yb_2Pt_3Sn_5$ Type Stannides (Space Group *Pnma*)

Compound	a (pm)	b (pm)	c (pm)	V (nm^3)	Reference
$Ca_2Pt_3Sn_5$[a]	734.8(1)	445.50(7)	2634.8(5)	0.8625(2)	(10)
$Ca_2Pt_3Sn_5$[b]	736.7(5)	444.7(1)	2640.5(6)	0.8651(1)	(10)
$CaErPt_3Sn_5$[a]	736.4(1)	444.11(9)	2639.9(4)	0.8634(4)	this work
$Ca_{1.33(1)}Er_{0.67(1)}Pt_3Sn_5$[b]	731.25(7)	442.62(4)	2628.9(3)	0.8509(1)	this work
$CaTmPt_3Sn_5$[a]	733.9(2)	443.0(1)	2634.8(5)	0.8566(4)	this work
$Ca_{1.45(1)}Tm_{0.55(1)}Pt_3Sn_5$[b]	732.13(9)	442.39(6)	2631.0(4)	0.8521(2)	this work
$CaYbPt_3Sn_5$[a]	733.9(1)	443.3(1)	2635.7(6)	0.8575(4)	this work
$Ca_{1.28(1)}Yb_{0.72(1)}Pt_3Sn_5$[b]	733.55(9)	443.23(6)	2634.1(4)	0.8565(2)	this work
$CaLuPt_3Sn_5$[a]	735.0(2)	441.6(2)	2634.1(7)	0.8550(4)	this work
$Ca_{1.63(1)}Lu_{0.37(1)}Pt_3Sn_5$[b]	734.27(8)	442.90(5)	2636.5(4)	0.8574(2)	this work
$Yb_2Pt_3Sn_5$	729.5(2)	442.2(1)	2625.2(6)	0.8468(4)	(6)

Note. Standard deviations in the positions of the last significant digits are given in parentheses.

[a] Guinier powder data. For the lanthanoid-containing compounds these lattice parameters were determined from samples which were prepared from starting compositions Ca : Ln : Pt : Sn = 1 : 1 : 3 : 5.

[b] These data were obtained on the four-circle diffractometer for a selected single crystal.

X-ray Investigations

The samples were routinely characterized through Guinier powder patterns with Cu$K\alpha_1$ radiation and α-quartz ($a = 491.30$ pm, $c = 540.46$ pm) as an internal standard. The orthorhombic lattice constants (Table 1) were obtained from least-squares fits of the Guinier powder data. To assure correct indexing, the observed patterns were compared with calculated ones (12), taking the atomic positions from the structure refinements. The lattice constants of a selected single crystal were determined on a four-circle diffractometer. These values are also listed in Table 1.

Single-crystal intensity data were collected at room temperature by use of a four-circle diffractometer (CAD4) with graphite monochromatized Mo$K\alpha$ radiation ($\lambda =$ 71.073 pm) and a scintillation counter with pulse height discrimination. The scans were performed in the $\omega/2\theta$ mode, and empirical absorption corrections were applied on the basis of psi-scan data.

Magnetic Measurements

The magnetic susceptibilities of polycrystalline pieces of all stannides were determined with a SQUID magnetometer (Quantum Design, Inc.) in the temperature range 2–300 K with magnetic flux densities up to 5.5 T.

Metallography

A sample of $CaTmPt_3Sn_5$ was embedded in a methacrylate matrix (Struers Acryfix) and polished with a diamond paste. The microstructure of the unetched surface was analyzed in a Leica 420 I scanning electron microscope in backscattering mode. Energy dispersive analyses of X-rays (EDX) were taken with wollastonite, tin, TmF_3, and platinum as standards.

RESULTS AND DISCUSSION

Synthesis, Lattice Parameters, and Homogeneity Ranges

All samples were prepared from the intended compositions Ca : Ln : Pt : Sn = 1 : 1 : 3 : 5. The structure refinements, however, indicated that a mixed occupancy of the cationic sites occurs. The degree of calcium–rare-earth mixing will certainly vary from crystal to crystal. The mixed occupancies are thus also expressed in the values of the lattice parameters. As is evident from Table 1, the lattice parameters determined from the Guinier powder data deviate from the single-crystal data. In view of the mixed occupancies, however, this is comprehensible. The powder lattice parameters decrease from the erbium to the lutetium compound as expected from the lanthanoid contraction. The ytterbium compound $CaYbPt_3Sn_5$ shows a positive deviation from this behavior due to the mixed-valent character of the ytterbium atoms. Surprisingly, the cell volume of the erbium compound is as large as that of the pure calcium compound. We attribute this slight enlargement of the cell to the mixed Ca/Er occupancy. However, considering the atomic radii, one would expect a slightly smaller cell volume for the erbium compound.

The microstructure of the $CaTmPt_3Sn_5$ sample was analyzed by EDX in more detail. The surface showed two

TABLE 2
Crystal Data and Structure Refinements for $Ca_{1.33}Er_{0.67}Pt_3Sn_5$, $Ca_{1.45}Tm_{0.55}Pt_3Sn_5$, $Ca_{1.28}Yb_{0.72}Pt_3Sn_5$, and $Ca_{1.63}Lu_{0.37}Pt_3Sn_5$ ($Z = 4$, Space Group *Pnma*, oP40)

Empirical formula:	$Ca_{1.33}Er_{0.67}Pt_3Sn_5$	$Ca_{1.45}Tm_{0.55}Pt_3Sn_5$	$Ca_{1.28}Yb_{0.72}Pt_3Sn_5$	$Ca_{1.63}Lu_{0.37}Pt_3Sn_5$
Molar mass (g/mol)	1344.09	1329.75	1354.61	1308.79
Calculated density (g/cm^3)	10.66	10.76	10.78	10.83
Crystal size (μm^3)	$10 \times 20 \times 40$	$20 \times 50 \times 75$	$50 \times 15 \times 20$	$15 \times 25 \times 55$
Transm. ratio (max/min)	3.33	6.79	2.32	4.07
Abs. coefficient (mm^{-1})	72.7	73.8	74.3	75.2
$F(000)$	2288	2292	2296	2300
θ range for data collection	2° to 30°	2° to 30°	2° to 35°	2° to 30°
Range in *hkl*	$\pm 10, \pm 6, \pm 37$	$\pm 10, \bar{6} < k < 0, \pm 37$	$\overline{11} < h < 10, \bar{7} < k < 0, \pm 42$	$0 < h < 10, 0 < k < 6, \pm 37$
Total no. of reflections	9408	5111	6688	2640
Independent reflections	1403 ($R_{int} = 0.079$)	1372 ($R_{int} = 0.054$)	2079 ($R_{int} = 0.062$)	1344 ($R_{int} = 0.039$)
Reflections with $I > 2\sigma(I)$	1007($R_{sigma} = 0.039$)	1114 ($R_{sigma} = 0.039$)	1520 ($R_{sigma} = 0.055$)	1088 ($R_{sigma} = 0.046$)
Data/restraints/parameters	1403/0/63	1372/0/63	2079/0/64	1344/0/63
Goodness-of-fit on F^2	1.232	1.078	1.098	1.010
Final R indices [$I > 2\sigma(I)$]	$R1 = 0.0330$	$R1 = 0.0419$	$R1 = 0.0294$	$R1 = 0.0440$
	$wR2 = 0.0722$	$wR2 = 0.1195$	$wR2 = 0.0583$	$wR2 = 0.1123$
R indices (all data)	$R1 = 0.0694$	$R1 = 0.0613$	$R1 = 0.0632$	$R1 = 0.0596$
	$wR2 = 0.0905$	$wR2 = 0.1430$	$wR2 = 0.0734$	$wR2 = 0.1202$
Extinction coefficient	0.00007(5)	0.0011(1)	0.00018(3)	0.0007(1)
Largest diff. peak and hole	5.27 and -4.68 e/Å^3	4.67 and -7.57 e/Å^3	4.98 and -4.96 e/Å^3	5.59 and -6.28 e/Å^3

Note. The $F(000)$ values were calculated for the ideal formulae. The molar masses and the calculated densities correspond to the refined compositions.

different phases which could be distinguished by their slightly varying gray color.

The EDX analyses showed compositions (in atomic %) of 16 ± 2 Ca : 6 ± 2 Tm : 29 ± 2 Pt : 49 ± 2 Sn and 12 ± 2 Ca : 11 ± 2 Tm : 27 ± 2 Pt : 50 ± 2 Sn for these two phases, clearly indicating a homogeneity range. The large standard deviation accounts for the results obtained for several spot analyses. Such small homogeneity ranges are also expected for the other samples.

Structure Refinements

Platelet-like single crystals of the four stannides were isolated from the annealed samples by mechanical fragmentation and were examined by Buerger precession photographs in order to establish symmetry and suitability for intensity data collection. The photographs showed primitive orthorhombic cells and the extinction conditions were compatible with space group *Pnma* (No. 62) in agreement with the previous investigations on $Yb_2Pt_3Sn_5$ (6) and $Ca_2Pt_3Sn_5$ (10). All relevant crystallographic data and details for the data collections are listed in Table 2.

The atomic positions of $Ca_2Pt_3Sn_5$ (10) were taken as starting values, and the structures were successfully refined using SHELXL-97 (full-matrix least-squares on F^2) (13) with anisotropic displacement parameters for all atoms. The course of the equivalent isotropic displacement parameters readily indicated a mixed occupancy of the M2 site in the erbium, thulium, and lutetium compound, and even a mixed occupancy for both cationic positions in the ytterbium compound. The respective sites were then refined with mixed calcium–rare-earth occupancy with the values listed in Table 3. As a further check for the correct composition, all other occupancy parameters were refined in separate series of least-squares cycles. Within two standard deviations, no deviations from full occupancy were observed, and we can therefore exclude tin–platinum mixing in the structure. In the final cycles, only the occupancy parameters of the respective M sites were allowed to vary. The refinements then converged to the residuals listed in Table 3. Final difference Fourier synthesis revealed no significant residual peaks. The highest residual densities were all close to the platinum positions and most likely resulted from incomplete absorption corrections of these strongly absorbing compounds. The positional parameters and interatomic distances of the four refinements are listed in Tables 3 and 4. Listings of the observed and calculated structure factors are available.[1]

Crystal Chemistry

The new stannides $CaErPt_3Sn_5$, $CaTmPt_3Sn_5$, $CaYbPt_3Sn_5$, and $CaLuPt_3Sn_5$ are new representatives of

[1] Details may be obtained from Fachinformationszentrum Karlsruhe, D-76344 Eggenstein-Leopoldshafen (Germany), by quoting the Registry No's. CSD-410966 ($CaErPt_3Sn_5$), CSD-410965 ($CaTmPt_3Sn_5$), CSD-410964 ($CaYbPt_3Sn_5$), and CSD-410963 ($CaLuPt_3Sn_5$).

TABLE 3

Atomic Coordinates and Isotropic Displacement Parameters (pm^2) for $Ca_{1.33}Er_{0.67}Pt_3Sn_5$, $Ca_{1.45}Tm_{0.55}Pt_3Sn_5$, $Ca_{1.28}Yb_{0.72}Pt_3Sn_5$, and $Ca_{1.63}Lu_{0.37}Pt_3Sn_5$

Atom	Occupancy	x	z	U_{eq}
		$Ca_{1.33}Er_{0.67}Pt_3Sn_5$		
Ca	0.99(2)	0.2495(6)	0.5769(2)	141(9)
M2	0.33(1) Ca + 0.67(1) Er	0.2182(2)	0.27261(5)	77(4)
Pt1	0.99(1)	0.5024(1)	0.70163(3)	82(2)
Pt2	1.00(1)	0.9665(1)	0.35625(3)	79(2)
Pt3	1.00(1)	0.7429(1)	0.52781(3)	79(2)
Sn1	0.98(1)	0.1211(2)	0.70115(5)	72(3)
Sn2	1.02(1)	0.5925(2)	0.34727(6)	80(3)
Sn3	1.00(1)	0.7831(2)	0.63096(5)	82(3)
Sn4	1.00(1)	0.4645(2)	0.45631(6)	80(3)
Sn5	0.99(1)	0.0375(2)	0.45660(6)	88(3)
		$Ca_{1.45}Tm_{0.55}Pt_3Sn_5$		
Ca	0.96(3)	0.2485(6)	0.5765(2)	142(10)
M2	0.45(1) Ca + 0.55(1) Tm	0.2176(2)	0.27286(6)	94(5)
Pt1	1.01(1)	0.5025(1)	0.70146(4)	98(3)
Pt2	1.01(1)	0.9661(1)	0.35655(4)	92(3)
Pt3	1.00(1)	0.7430(1)	0.52776(4)	90(3)
Sn1	0.99(1)	0.1214(2)	0.70135(6)	74(3)
Sn2	1.01(1)	0.5930(2)	0.34728(7)	90(3)
Sn3	1.01(1)	0.7836(2)	0.63078(6)	91(3)
Sn4	0.99(1)	0.4646(2)	0.45657(6)	92(3)
Sn5	0.99(1)	0.0377(2)	0.45648(6)	100(4)
		$Ca_{1.28}Yb_{0.72}Pt_3Sn_5$		
M1	0.74(1) Ca + 0.26(1) Yb	0.2489(2)	0.57669(6)	125(4)
M2	0.54(1) Ca + 0.46(1) Yb	0.2167(1)	0.27286(4)	88(3)
Pt1	1.00(1)	0.50132(6)	0.70086(2)	87(1)
Pt2	1.00(1)	0.96364(6)	0.35705(2)	81(1)
Pt3	0.99(1)	0.74315(6)	0.52767(2)	82(1)
Sn1	1.00(1)	0.1211(1)	0.70160(3)	70(2)
Sn2	1.01(1)	0.5926(1)	0.34709(3)	82(2)
Sn3	0.99(1)	0.7852(1)	0.63109(3)	81(2)
Sn4	1.00(1)	0.4640(1)	0.45644(3)	76(2)
Sn5	1.00(1)	0.0390(1)	0.45677(3)	80(2)
		$Ca_{1.63}Lu_{0.37}Pt_3Sn_5$		
Ca	1.00(1)	0.2490(6)	0.5766(2)	124(9)
M2	0.63(1) Ca + 0.37(1) Lu	0.2163(2)	0.27318(7)	88(6)
Pt1	1.00(1)	0.5025(1)	0.70114(3)	94(2)
Pt2	1.00(1)	0.9634(1)	0.35703(3)	85(2)
Pt3	1.01(1)	0.7431(1)	0.52764(3)	79(2)
Sn1	1.00(1)	0.1224(2)	0.70149(6)	68(3)
Sn2	1.02(1)	0.5920(2)	0.34687(6)	78(3)
Sn3	0.98(1)	0.7848(2)	0.63086(6)	85(3)
Sn4	1.00(1)	0.4636(2)	0.45637(6)	76(3)
Sn5	0.99(1)	0.0396(2)	0.45661(6)	78(3)

Note. U_{eq} is defined as one-third of the trace of the orthogonalized U_{ij} tensor. The positions denoted M1 and M2 show mixed rare-earth–calcium occupancy as indicated in the second row. All atoms occupy the Wyckoff site 4*c* ($x1/4z$) of space group *Pnma*. The occupancy parameters were obtained in a separate series of least-square cycles. In the final cycles, only the occupancies of the M1 and M2 sites were allowed to vary.

the $Yb_2Pt_3Sn_5$ type structure (6), which has also been observed for $Ca_2Pt_3Sn_5$ (10). Although the structure refinements revealed mixed calcium–rare-earth occupancy with relatively complex chemical compositions (Table 3), we use the idealized formulae in the following discussion.

Since the crystal chemistry of the $Yb_2Pt_3Sn_5$ type stannides was already discussed in detail in Refs. (6) and (10), we give only a brief account here. As outlined in Fig. 1, the structure of these stannides is built up from a complex three-dimensional $[Pt_3Sn_5]$ polyanion in which the calcium and rare-earth atoms fill distorted pentagonal and hexagonal channels. Extended-Hückel calculations for isotypic $Ca_2Pt_3Sn_5$ (10) indicated strongly bonding Pt–Sn and Sn–Sn interactions within the polyanionic network, while the Ca–Pt and Ca–Sn overlap populations were about one order of magnitude smaller. These results are compatible with a formulation $(2Ca^{2+})^{4+}$ $[Pt_3Sn_5]^{4-}$, assuming a full charge transfer from the calcium atoms to the polyanion. Our previous investigations of the magnetic susceptibility of $Yb_2Pt_3Sn_5$, however, showed mixed valent behavior of the ytterbium atoms (6). From the experimental magnetic moment of 2.6(1) μ_B/Yb, it was evident that about one-half of the ytterbium atoms would be in the trivalent oxidation state leading to a formulation $(Yb1^{2+})(Yb2^{3+})$ $[Pt_3Sn_5]^{5-}$. Thus, the $[Pt_3Sn_5]$ network has a certain flexibility for the electron count.

The two crystallographically different M (calcium and rare-earth metal) atoms have distinctly different coordinations (Fig. 2). M1 has coordination number (CN) 20 with 2 M1, 7 Pt, and 11 Sn atoms in the coordination shell, while the M2 atoms have only CN 18 with 4 M2, 6 Pt, and 8 Sn neighbors. For the pure ytterbium compound (6) we assumed an occupancy of the M1 polyhedron by the larger Yb^{2+} cations, while the smaller Yb^{3+} cations fill the M2 polyhedron. This is essentially confirmed by the four structure refinements of the rare-earth- and calcium-containing compounds.

With erbium, thulium, and lutetium as rare earth components we find a full occupancy with calcium on the M1 site and a mixed rare-earth–calcium occupancy on the M2 site, clearly indicating a site preference for the larger divalent cation on the M1 site. The mixed occupancy on the M2 site is not surprising, since the pure calcium stannide $Ca_2Pt_3Sn_5$ also exists (10). The M1 site, however, is most likely too large for the trivalent rare-earth cations. A mixed occupancy of this site can definitely be excluded for the single crystals investigated, since the refined occupancy parameters never exceeded 1.00 (Table 3). In contrast, a mixed calcium–ytterbium occupancy was observed for the ytterbium-based stannides. Here, the ytterbium atoms show mixed valent behavior (see magnetic data below) and therefore can match the size within both coordination polyhedra.

TABLE 4
Interatomic Distances (pm), Calculated with the Lattice Constants Taken from X-Ray Powder Data of $Ca_{1.33}Er_{0.67}Pt_3Sn_5$, $Ca_{1.45}Tm_{0.55}Pt_3Sn_5$, $Ca_{1.28}Yb_{0.72}Pt_3Sn_5$, and $Ca_{1.63}Lu_{0.37}Pt_3Sn_5$

$Ca_{1.33}Er_{0.67}Pt_3Sn_5$				$Ca_{1.45}Tm_{0.55}Pt_3Sn_5$				$Ca_{1.28}Yb_{0.72}Pt_3Sn_5$				$Ca_{1.63}Lu_{0.37}Pt_3Sn_5$			
Ca:	2	Sn4	318.4	Ca:	2	Sn5	317.4	M1:	2	Sn4	318.0	Ca:	2	Sn4	317.7
	2	Sn5	319.0		2	Sn4	317.8		2	Sn5	318.7		2	Sn5	318.5
	2	Sn2	320.9		2	Sn2	320.8		2	Sn2	321.0		2	Sn2	321.0
	2	Pt2	325.2		2	Pt2	324.0		2	Pt2	322.4		2	Pt2	322.0
	1	Sn1	341.5		1	Sn1	341.8		1	Sn1	342.3		1	Sn1	341.9
	1	Sn5	353.8		1	Sn5	352.1		1	Sn5	351.6		1	Sn5	351.6
	2	Pt3	354.5		2	Pt3	353.0		2	Pt3	353.3		2	Pt3	352.4
	1	Sn4	355.5		1	Sn4	353.6		1	Sn4	354.1		1	Sn4	353.8
	1	Sn3	372.0		1	Sn3	369.9		1	Sn3	369.3		1	Sn3	369.9
	1	Pt1	378.4		1	Pt1	378.2		1	Pt1	376.1		1	Pt1	377.2
	1	Pt3	385.7		1	Pt3	385.0		1	Pt3	385.0		1	Pt3	385.4
	1	Pt3	394.9		1	Pt3	392.6		1	Pt3	393.0		1	Pt3	393.6
	1	Sn3	418.1		1	Sn3	417.9		1	Sn3	418.9		1	Sn3	418.9
	2	Ca	444.1		2	Ca	443.0		2	M1	443.3		2	Ca	441.6
M2:	1	Pt2	288.3	M2:	1	Pt2	287.6	M2:	1	Pt2	289.4	M2:	1	Pt2	288.7
	2	Pt1	310.3		2	Pt1	309.6		2	Pt1	311.1		2	Pt1	310.0
	2	Sn1	314.5		2	Sn1	313.9		2	Sn1	314.0		2	Sn1	313.8
	1	Sn2	329.7		1	Sn2	329.5		1	Sn2	329.0		1	Sn2	329.2
	2	Pt1	332.9		2	Pt1	332.5		2	Pt1	332.8		2	Pt1	332.6
	2	Sn3	337.8		2	Sn3	336.9		2	Sn3	336.5		2	Sn3	335.6
	1	Sn2	338.9		1	Sn2	338.2		1	Sn2	338.2		1	Sn2	337.6
	2	Sn1	341.4		2	Sn1	340.0		2	Sn1	339.3		2	Sn1	339.4
	1	Pt2	386.2		2	M2	386.2		2	M2	386.2		2	M2	387.3
	2	M2	387.1		1	Pt2	386.7		1	Pt2	387.5		1	Pt2	388.1
	2	M2	444.1		2	M2	443.0		2	M2	443.3		2	M2	441.6
Pt1:	2	Sn2	266.2	Pt1:	2	Sn2	265.4	Pt1:	2	Sn2	264.3	Pt1:	2	Sn2	263.8
	1	Sn1	271.1		1	Sn1	270.6		1	Sn1	271.7		1	Sn1	271.2
	1	Sn3	278.4		1	Sn3	278.0		1	Sn3	277.9		1	Sn3	278.1
	1	Sn1	280.8		1	Sn1	279.7		1	Sn1	279.0		1	Sn1	279.3
	2	M2	310.3		2	M2	309.6		2	M2	311.1		2	M2	310.0
	2	M2	332.9		2	M2	332.5		2	M2	332.8		2	M2	332.6
	1	Ca	378.4		1	Ca	378.2		1	M1	376.1		1	Ca	377.2
Pt2:	1	Sn5	270.1	Pt2:	1	Sn5	268.5	Pt2:	1	Sn5	268.6	Pt2:	1	Sn5	268.2
	1	Sn2	276.4		1	Sn2	274.9		1	Sn2	273.6		1	Sn2	274.3
	2	Sn1	276.5		2	Sn1	276.5		2	Sn1	277.3		2	Sn1	276.6
	1	M2	288.3		1	M2	287.6		1	M2	289.4		1	M2	288.7
	2	Sn3	290.7		2	Sn3	289.7		2	Sn3	290.0		2	Sn3	289.9
	2	Ca	325.2		2	Ca	323.9		2	M1	322.4		2	Ca	322.0
	1	M2	386.2		1	M2	386.7		1	M2	387.5		1	M2	388.1
Pt3:	2	Sn4	272.7	Pt3:	2	Sn4	272.0	Pt3:	2	Sn4	272.0	Pt3:	2	Sn4	271.3
	1	Sn3	273.9		1	Sn3	273.1		1	Sn3	274.3		1	Sn3	273.6
	2	Sn5	277.8		2	Sn5	276.9		2	Sn5	276.4		2	Sn5	275.6
	1	Sn4	278.7		1	Sn4	277.4		1	Sn4	277.9		1	Sn4	278.3
	1	Sn5	287.1		1	Sn5	286.4		1	Sn5	286.5		1	Sn5	287.2
	2	Ca	354.5		2	Ca	353.0		2	M1	353.3		2	Ca	352.4
	1	Ca	385.7		1	Ca	385.0		1	M1	385.0		1	Ca	385.4
	1	Ca	394.9		1	Ca	392.6		1	M1	393.0		1	Ca	393.6
Sn1:	1	Pt1	271.1	Sn1:	1	Pt1	270.6	Sn1:	1	Pt1	271.7	Sn1:	1	Pt1	271.2
	2	Pt2	276.5		2	Pt2	276.5		2	Pt2	277.3		2	Pt2	276.6
	1	Pt1	280.8		1	Pt1	279.7		1	Pt1	279.0		1	Pt1	279.3
	1	Sn3	310.3		1	Sn3	309.9		1	Sn3	308.8		1	Sn3	310.2
	2	M2	314.5		2	M2	313.9		2	M2	314.0		2	M2	313.8
	2	Sn2	331.8		2	Sn2	330.8		2	Sn2	331.3		2	Sn2	330.2
	2	M2	341.4		2	M2	340.0		2	M2	339.3		2	M2	339.4
	1	Ca	341.5		1	Ca	341.8		1	M1	342.3		1	Ca	341.9

TABLE 4—*Continued*

$Ca_{1.33}Er_{0.67}Pt_3Sn_5$				$Ca_{1.45}Tm_{0.55}Pt_3Sn_5$				$Ca_{1.28}Yb_{0.72}Pt_3Sn_5$				$Ca_{1.63}Lu_{0.37}Pt_3Sn_5$			
Sn2:	2	Pt1	266.2	Sn2:	2	Pt1	265.4	Sn2:	2	Pt1	264.3	Sn2:	2	Pt1	263.8
	1	Pt2	276.4		1	Pt2	274.9		1	Pt2	273.6		1	Pt2	274.3
	1	Sn4	302.9		1	Sn4	303.0		1	Sn4	303.3		1	Sn4	303.5
	2	Ca	320.9		2	Ca	320.8		2	M1	321.0		2	Ca	321.0
	1	M2	329.7		1	M2	329.5		1	M2	329.0		1	M2	329.2
	2	Sn1	331.8		2	Sn1	330.8		2	Sn1	331.3		2	Sn1	330.2
	1	M2	338.9		1	M2	338.2		1	M2	338.2		1	M2	337.6
	2	Sn3	359.3		2	Sn3	358.9		2	Sn3	359.6		2	Sn3	359.0
Sn3:	1	Pt3	273.9	Sn3:	1	Pt3	273.1	Sn3:	1	Pt3	274.3	Sn3:	1	Pt3	273.6
	1	Pt1	278.4		1	Pt1	278.0		1	Pt1	277.9		1	Pt1	278.1
	2	Pt2	290.7		2	Pt2	289.7		2	Pt2	290.0		2	Pt2	290.0
	1	Sn1	310.4		1	Sn1	309.9		1	Sn1	308.8		1	Sn1	310.1
	2	M2	337.8		2	M2	336.9		2	M2	336.5		2	M2	335.6
	2	Sn5	346.7		2	Sn5	345.1		2	Sn5	345.6		2	Sn5	344.2
	2	Sn2	359.3		2	Sn2	358.9		2	Sn2	359.6		2	Sn2	359.0
	2	Sn4	368.3		2	Sn4	367.7		2	Sn4	368.5		2	Sn4	367.3
	1	Ca	372.0		1	Ca	369.9		1	M1	369.3		1	Ca	369.9
	1	Ca	418.1		1	Ca	417.9		1	M1	418.9		1	Ca	418.9
Sn4:	2	Pt3	272.7	Sn4:	2	Pt3	272.0	Sn4:	2	Pt3	272.0	Sn4:	2	Pt3	271.3
	1	Pt3	278.7		1	Pt3	277.4		1	Pt3	277.9		1	Pt3	278.3
	1	Sn2	302.9		1	Sn2	303.0		1	Sn2	303.3		1	Sn2	303.5
	1	Sn5	314.4		1	Sn5	313.3		1	Sn5	311.9		1	Sn5	311.7
	2	Ca	318.4		2	Ca	317.8		2	M1	318.0		2	Ca	317.7
	2	Sn4	324.4		2	Sn4	322.7		2	Sn4	323.5		2	Sn4	323.2
	1	Ca	355.5		1	Ca	353.6		1	M1	354.1		1	Ca	353.8
	2	Sn3	368.3		2	Sn3	367.7		2	Sn3	368.5		2	Sn3	367.3
Sn5:	1	Pt2	270.0	Sn5:	1	Pt2	268.5	Sn5:	1	Pt2	268.6	Sn5:	1	Pt2	268.2
	2	Pt3	277.8		2	Pt3	276.9		2	Pt3	276.4		2	Pt3	275.6
	1	Pt3	287.1		1	Pt3	286.4		1	Pt3	286.5		1	Pt3	287.2
	1	Sn4	314.4		1	Sn4	313.3		1	Sn4	311.9		1	Sn4	311.7
	2	Ca	319.0		2	Ca	317.4		2	M1	318.7		2	Ca	318.5
	2	Sn5	323.8		2	Sn5	323.6		2	Sn5	323.0		2	Sn5	323.1
	2	Sn3	346.7		2	Sn3	345.1		2	Sn3	345.6		2	Sn3	344.2
	1	Ca	353.8		1	Ca	352.1		1	M1	351.6		1	Ca	351.6

Note. Standard deviations are all equal to or less than 0.5 pm. All distances within the first coordination spheres are listed. The sites M1 and M2 show mixed rare-earth–calcium occupancy (see also Table 3).

Magnetic Measurements

The temperature dependence of the inverse magnetic susceptibility of $CaErPt_3Sn_5$, $CaTmPt_3Sn_5$, and $CaYbPt_3Sn_5$, and the susceptibility of $CaLuPt_3Sn_5$ are presented in Figure 3. Since the $CaLnPt_3Sn_5$ stannides show small homogeneity ranges, it is certainly difficult to calculate reliable magnetic moments from the experimental data. The values listed in the following paragraphs have been calculated assuming the idealized fomulae $CaLnPt_3Sn_5$. The relatively high standard deviations of the magnetic moments account for the values obtained for different samples. Since the homogeneity ranges are only small, the deduced magnetic data are reliable within the standard deviations.

The erbium and the thulium stannide show Curie–Weiss behavior above 50 K with experimental magnetic moments (per formula unit) of 9.5(2) μ_B/f.u. (erbium) and 8.4(2) μ_B/f.u. (thulium). While the experimental moment of the erbium compound agrees well with the free ion value of 9.58 μ_B for Er^{3+}, the one for the thulium compound is higher than the free ion value of 7.56 μ_B for Tm^{3+}. The latter effect can solely be attributed to a partial occupancy (about 10%) of the calcium site by thulium atoms in the bulk sample. The EDX results (see above) also indicated such homogeneity ranges. The paramagnetic Curie temperatures (Weiss constants) of $\Theta = -3(2)$ K (erbium) and $\Theta = -1(2)$ K (thulium) were obtained by linear extrapolation of the high-temperature part (above 100 K) of the $1/\chi$ vs T plots to $1/\chi = 0$.

The inserts in Fig. 3 suggest magnetic ordering at low temperature. This was investigated in more detail for both stannides by low-temperature low-field measurements as

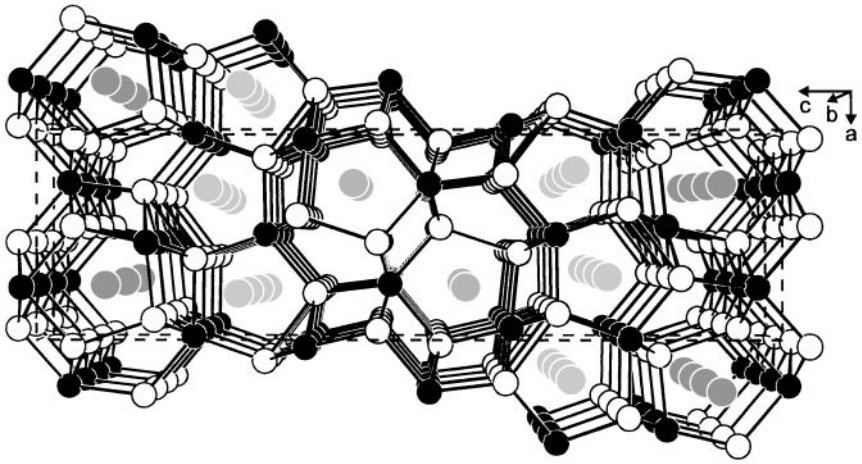

FIG. 1. Perspective view of the $CaErPt_3Sn_5$ structure along the *y* axis. The calcium, erbium, platinum, and tin atoms are drawn as light gray, medium gray, black, and open circles, respectively. The three-dimensional infinite $[Pt_3Sn_5]$ polyanion is emphasized.

outlined in Fig. 4. The zero-field and field-cooling (kink point measurement) curves of the erbium compound suggest ferro- or ferrimagnetic ordering. The precise ordering temperature of 4.7(1) K was determined from the derivative $d\chi/dT$ (insert in Fig. 4). Similar measurements of the thulium stannide indicate antiferromagnetic ordering at 5.0(1) K. The magnetic behavior of these two stannides was further studied by magnetization measurements (Fig. 5). At 50 K, well above the magnetic ordering temperatures, the magnetization curves are almost linear, as expected for a paramagnetic material. Slightly below the ordering temperatures, at 2 K, the magnetization curves show a steeper increase. At the highest obtainable field strength of 5.5 T the magnetizations are $\mu_{sm(exp)} = 4.8(2)\ \mu_B$/f.u. for the erbium and 5.2(2) μ_B/f.u. for the thulium compound and are significantly reduced, when compared with the maximal possible values of $\mu_{sm(calc)} = 9.0$ for Er^{3+} and 7.0 for Tm^{3+}. From the course of the magnetization curve, it can not definitely be concluded whether the erbium compound orders ferro- or ferrimagnetically. Although, $CaTmPt_3Sn_5$ orders antiferromagnetically at 0.002 T ($\equiv$ 20 G), the shape of the magnetization curve is similar to the erbium compound. Most likely a metamagnetic (antiparallel-to-parallel spin alignment) or spin–flop transition occurs at very low fields (< 0.1 T).

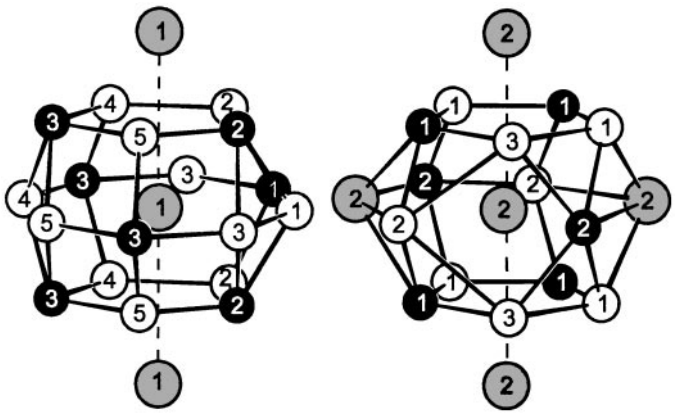

FIG. 2. Coordination polyhedra of the calcium and erbium atoms in $CaErPt_3Sn_5$. The dashed lines indicate the Ca–Ca and M–M distances corresponding to the lattice parameter *b*. The atom designations correspond to Fig. 1.

The magnetic properties of $CaYbPt_3Sn_5$ are similar to those of the pure ytterbium stannide $Yb_2Pt_3Sn_5$. $CaYbPt_3Sn_5$ shows Curie–Weiss behavior above 100 K (Fig. 3) with an experimental effective magnetic moment of 2.8(2) μ_B and a strongly negative Curie temperature of $-71(5)$ K. Both of these features are indicative of intermediate valence as already discussed in Ref. (6). The experimental moment is significantly smaller than the free ion value of 4.54 μ_B for Yb^{3+}. No magnetic ordering is detected down to 2 K. In agreement with the mixed-valent behavior of the ytterbium atoms, the magnetization curves at 2 and 50 K (Fig. 5) show only a slight curvature and very small magnetic moments. This was already the case for $Yb_2Pt_3Sn_5$ (6). The change in slope of the inverse susceptibility below 100 K is most likely a tendency of the ytterbium atoms towards the divalent state (the Curie temperature increases and the magnetic moment decreases). The ytterbium valence is thus strongly temperature dependent at low temperature.

The lutetium compound shows a diamagnetic signal over the whole temperature range (Fig. 3), with a room temperature value of -7.8×10^{-9} m^3/mol. At first sight, one may think that $CaLuPt_3Sn_5$ is a diamagnet. This, however, is in

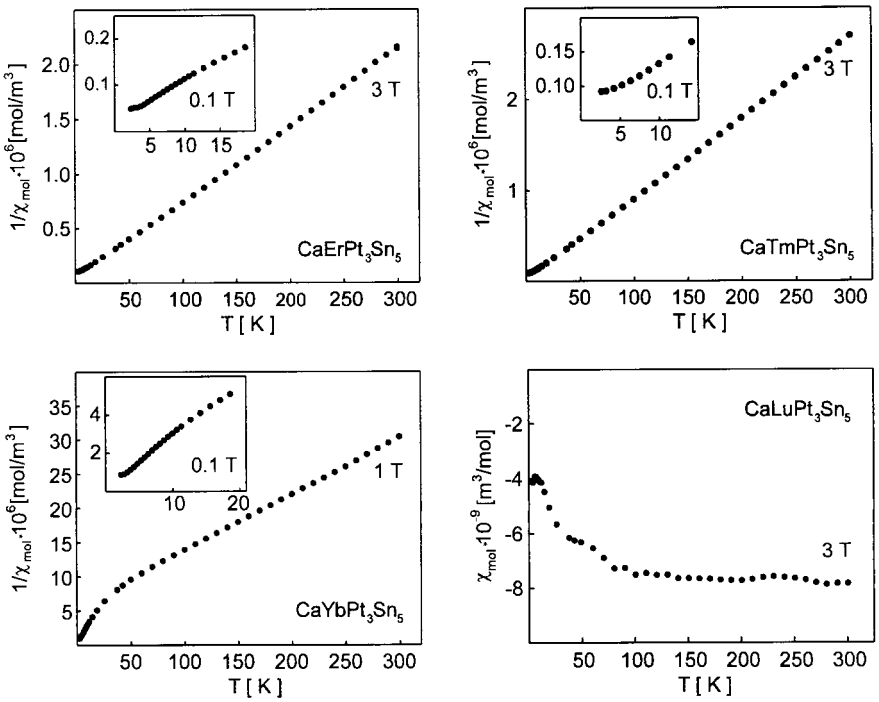

FIG. 3. Temperature dependence of the inverse magnetic susceptibilities of, respectively, $CaErPt_3Sn_5$, $CaTmPt_3Sn_5$, $CaYbPt_3Sn_5$, and $CaLuPt_3Sn_5$ measured at an external field of 3 T (at 1 T for the ytterbium compound). The behavior at low temperature and low external fields (0.1 T) is shown in the inserts.

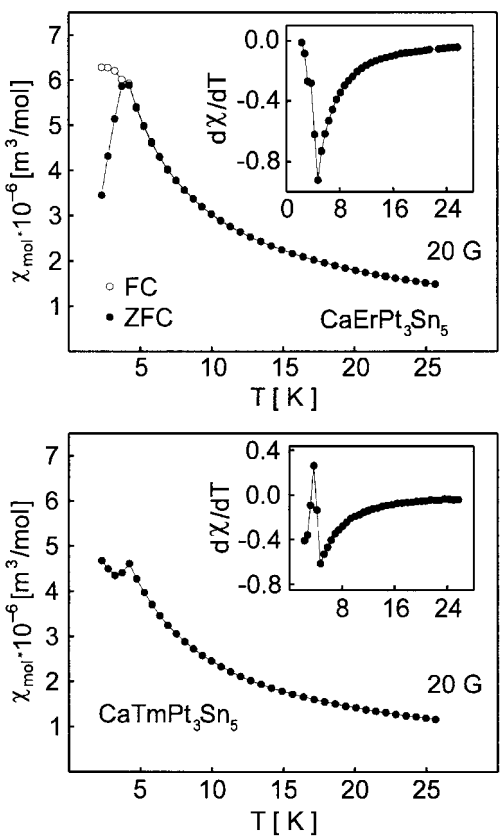

contrast with the nonvanishing DOS of $Ca_2Pt_3Sn_5$ and the metallic conductivity of $Yb_2Pt_3Sn_5$. Since the slightly higher electron count of $CaLuPt_3Sn_5$ pushes the Fermi level up only a bit, $CaLuPt_3Sn_5$ should also be a metallic conductor. We assume that the Pauli contribution of the conduction electrons is only small, and the strongly intrinsic diamagnetism dominates the susceptibility behavior of $CaLuPt_3Sn_5$.

CONCLUSION

We have synthesized a series of new $Yb_2Pt_3Sn_5$ type stannides, i.e., $CaErPt_3Sn_5$, $CaTmPt_3Sn_5$, $CaYbPt_3Sn_5$, and $CaLuPt_3Sn_5$. These stannides have two crystallographically different cation positions. The structure refinements clearly indicate the preference of one site for the larger Ca^{2+} ions. This is confirmed also by magnetic susceptibility measurements.

FIG. 4. Temperature dependence of the susceptibility of $CaErPt_3Sn_5$ and $CaTmPt_3Sn_5$ measured at an external field of 20 G ($\equiv 0.002$ T). For the erbium compound, both the zero-field-cooling (ZFC) and field-cooling (FC) curves are shown. The inserts show the derivatives $d\chi/dT$ for the determination at the exact ordering temperatures.

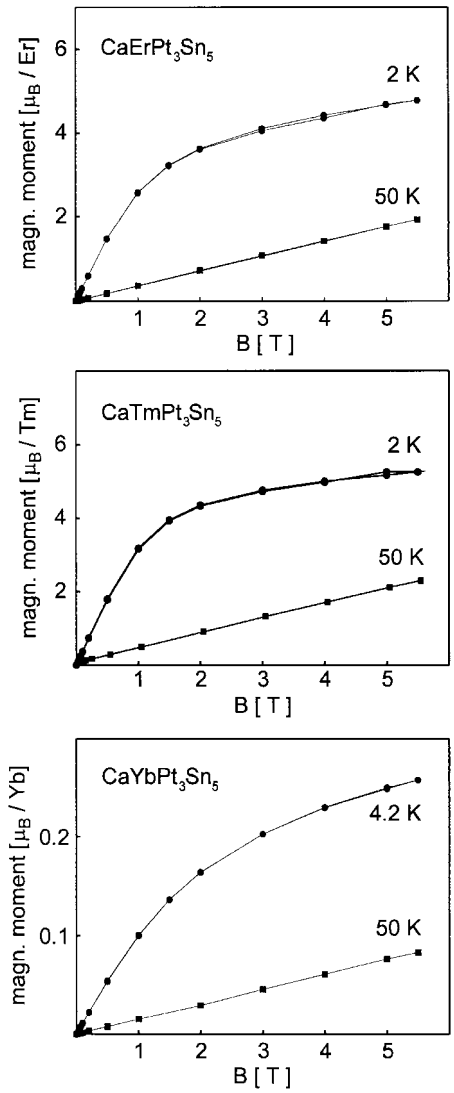

FIG. 5. Magnetization vs external magnetic flux density for $CaErPt_3Sn_5$, $CaTmPt_3Sn_5$, and $CaYbPt_3Sn_5$ at various temperatures.

ACKNOWLEDGMENTS

We are indebted to Professor W. Jeitschko for his interest and support of this work. The single-crystal data were competently measured by Dipl.-Ing. U. Ch. Rodewald. We also thank K. Wagner for the work at the scanning electron microscope and Dr. W. Gerhartz (Degussa AG) for a generous gift of platinum powder. This work was financially supported by the Deutsche Forschungsgemeinschaft and the Fond der Chemischen Industrie.

REFERENCES

1. A. Iandelli, A. Palenzona, and G. Olcese, *J. Less-Common Met.* **64,** 213 (1979).
2. R. Pöttgen, R.-D. Hoffmann, and D. Kußmann, *Z. Anorg. Allg. Chem.* **624,** 945 (1998).
3. E. V. Sampathkumaran, K. H. Frank, G. Kalkowski, G. Kaindl, M. Domke, and G. Wortmann, *Phys. Rev. B* **29,** 5702 (1984).
4. G. Cordier, T. Friedrich, R. Henseleit, A. Grauel, U. Tegel, C. Schank, and C. Geibel, *J. Alloys Compd.* **201,** 197 (1993).
5. C. Schank, U. Tegel, R. Henseleit, A. Grauel, G. Olesch, C. Geibel, G. Cordier, R. Kniep, and F. Steglich, *J. Alloys Compd.* **207/208,** 333 (1994).
6. R. Pöttgen, A. Lang, R.-D. Hoffmann, B. Künnen, G. Kotzyba, R. Müllmann, B. D. Mosel, and C. Rosenhahn, *Z. Kristallogr.* **214,** 143 (1999).
7. K. Katoh, T. Takabatake, A. Minami, I. Oguro, and H. Sawa, *J. Alloys Compd.* **261,** 32 (1997).
8. D. Kußmann, R. Pöttgen, B. Künnen, G. Kotzyba, R. Müllmann, and B. D. Mosel, *Z. Kristallogr.* **213,** 356 (1998).
9. R. Pöttgen, P. E. Arpe, C. Felser, D. Kußmann, R. Müllmann, B. D. Mosel, B. Künnen, and G. Kotzyba, *J. Solid State Chem.* **145,** 668 (1999).
10. R.-D. Hoffmann, D. Kußmann, U. Ch. Rodewald, R. Pöttgen, C. Rosenhahn, and B. D. Mosel, *Z. Naturforsch.* **54b,** 709 (1999).
11. D. Kußmann, R.-D. Hoffmann, and R. Pöttgen, *Z. Anorg. Allg. Chem.* **624,** 1727 (1998).
12. K. Yvon, W. Jeitschko, and E. Parthé, *J. Appl. Crystallogr.* **10,** 73 (1977).
13. G. M. Sheldrick, SHELXL-97, Program for Crystal Structure Refinement, University of Göttingen, 1997.